



Pristine graphene oxide treatment of wastewater from a typical sub-tropical mine in Chegutu, Zimbabwe

F. R. Kalitsilo¹ · H. Hashemi² · E. T. Mombeshora^{1,3}

Received: 13 September 2024 / Revised: 3 December 2024 / Accepted: 21 January 2025 / Published online: 7 February 2025
© The Author(s) 2025

Abstract

Mining activities in sub-tropical regions are one of the major contributors to environmental contamination and therefore require monitoring and mitigation methodologies. The study investigated the composition of the real-world wastewater from mine explosions and explored the potential of graphene oxide as an adsorbent. Heavy metals, namely, Fe (12.10 ppm), Cu (40.70 ppm), Cr (148 ppm) and Pb (0.03 ppm) were present. The optimal pH, adsorbent dose, temperature, and contact time for heavy metal removal were 12.08, 0.5 g, 25 °C and 0.5 h, respectively. The basic conditions were favourable for efficient removal through the adsorption method. Kinetic modelling indicated adsorption via pseudo-second-order kinetics, insinuating the influence of oxygen moieties of graphene oxide. Furthermore, the Langmuir isotherm revealed favourable removal of Fe, Cu, and Cr. The study indicated potential hazards of current mining activities, especially unmonitored illegal mines in sub-tropical regions. These findings highlight the prospects of graphene oxide as a practical and effective adsorbent for water resource recovery facilities. Therefore, the study demonstrated the capability to adopt pristine graphene oxide in a simple protocol using simple setups for wastewater recovery in the sub-tropical regions in a natural matrix.

Keywords Adsorption · Carbon · Energetic materials · Environmental sustainability · Explosives · Heavy metals

Introduction

The mining industry generates many pollutants that can contaminate water sources, posing significant risks to ecosystems and human health. Explosive blast mine effluent refers to wastewater generated during mining operations involving explosives (Bailey et al. 2013). This effluent can contain several heavy metals, such as Hg, Ni, Cd, As, Cr, and Pb (Ebenebe et al. 2018). These metals are commonly associated with mining activities due to their presence in

the ore deposits being extracted and, in some cases, in the explosives used. The discharge of heavy metals into the environment can occur through various pathways, including direct discharge of mine effluents into surface waters or infiltration into groundwater. Once released, heavy metals can persist in the surrounding environment for long periods and accumulate in sediments, plants, and animals. This accumulation can lead to certain hazards that may have adverse impacts on aquatic ecosystems and, in some cases, may also pose potential risks to human health if not properly managed (Liu et al. 2022a, b). The global community has been concerned about the various heavy metal ions in water bodies for many years, which are a significant risk to the aquatic environment, humans, and the environment. This is particularly concerning because these toxic heavy metals cannot be degraded and can enter the food chain, leading to serious public health issues and even deaths.

Therefore, explosive blast mine effluent requires qualitative and quantitative analyses to assess the environmental impact of mining activities. This provides valuable information to design appropriate mitigation measures, such as water resource recovery facilities to remove heavy metal contaminants. This is particularly important in the sub-tropical region context since

Editorial responsibility: S.Mirkia.

✉ E. T. Mombeshora
et.mombeshora@up.ac.za

¹ Department of Chemistry and Earth Sciences, University of Zimbabwe, Post Office Box MP167, Mount Pleasant, Harare, Zimbabwe

² Department of Chemical and Metallurgical Engineering, University of the Witwatersrand, Johannesburg WITS 2050, South Africa

³ Department of Chemistry, University of Pretoria, Private Bag X20, Hatfield 0028, Pretoria, South Africa



there are numerous mining activities which are both legal and illegal. Regulatory compliance is lacking in illegal mining; therefore, mining operations are mostly not subject to environmental regulations that limit the reckless act of discharging heavy metals into the environment (Radu et al. 2023). Qualitative and quantitative analysis ensures compliance with these regulations by identifying heavy metal sources and monitoring their concentrations in mine effluents to promote environmental sustainability.

Various methods for water resource recovery facilities, such as chemical precipitation (Zhang & Duan 2020), coagulation (El-taweel et al. 2023), photocatalysis (Borges et al. 2023) and adsorption (Peng et al. 2017) have been explored. Of all these methods, adsorption is more promising when considering cost-effectiveness from low energy input requirement, simplicity, easy integration into existing water resource recovery facilities, and superior removal efficiency (Dubey et al. 2015). Adsorption entails the adhesion of pollutants onto a solid surface, thus effectively removing contaminants from the water. This method has received more attention among other efficient options because of its non-hazardous, straightforward, and versatile nature.

A variety of adsorbent materials, including chitosan (Mishra et al. 2023), activated carbon (Cordova Estrada et al. 2021), zeolites (Maharana & Sen 2021), clay minerals (ElBastamy et al. 2021) and biochar (Obey et al. 2022) have been reported for water resource recovery facilities. Extensive application of these traditional sorbents in environmental remediation is hindered by their low efficacy, particularly for the removal of heavy metals (Wang 2012). Nanomaterials have shown great potential for this role, and graphene oxide (GO) is a typical material under intense research. GO is a derivative of graphene and has gained immense attention in different fields of study for its exceptional mechanical strength, chemical stability, flexibility, lightweight and high surface area, water solubility, and solution processability due to the abundance of oxygen-containing functionalities (OH, COOH, and C=O), on its surface (Mombeshora & Muchuweni 2023). Unique surface chemical characteristics and high surface area facilitate enhanced adsorbent/metal adhesion (Anegbe et al. 2024), thus, making GO a versatile material for water resource recovery facilities.

For example, GO has also been reported to exhibit excellent adsorption capacity toward organic compounds, including phenols and dyes (Jahan et al. 2022). Possible adsorption mechanisms include physical adsorption through weak van der Waals forces between the contaminant molecules and the GO surface. Physical adsorption is feasible for contaminants with large or easily polarisable electron clouds (Mahdhi et al. 2023). Furthermore, π - π interactions among the aromatic rings of certain organic contaminants and the π system of GO can lead to stronger adsorption forces (Zhang et al. 2022). Furthermore, OH and COOH moieties on GO form hydrogen bonds with contaminants containing suitable donor and acceptor sites

(Jahan et al. 2022). Finally, the pH of the solution may induce electrostatic interactions based on the surface charge of GO (Mishra et al. 2023).

Several works involving the removal of metallic contaminants involving GO have been reported. For example, both graphite powder and GO nanosheets were reported in the elimination of methylene blue dye and Cd^{2+} from water from an artificial matrix made by spiking (Cao et al. 2023). The adsorption equilibriums for both materials were reached after 0.83 h at room temperature and the removal efficacy of GO was better than that of graphite powder with maximum equilibrium adsorption capacity (q_e) of 24 and $\sim 13 \text{ mg g}^{-1}$, respectively. The application of GO composites in water resource recovery facilities has also been reported. For example; Cu, Cd, Pb and Zn ions which were spiked in a water solution were eliminated by using GO hydrogels, which were made by cross-linking GO with acrylamide and acrylic acid (Liu et al. 2023). The GO hydrogels were cost-effective, reusable in three cycles, and stable, and efficient adsorbent material for treating metal ions in water solutions. Sitko et al. (Sitko et al. 2016) used a cellulose-GO hydrogel to remove Cu^{2+} and Pb^{2+} from a spiked aqueous solution and deduced that adsorption increased considerably with adsorbent dose and achieved q_e of 27 and 108 mg g^{-1} at equilibrium at pH 4.8. Najafi et al. (Najafi et al. 2015) reported a decrease in Ni^{2+} adsorption in the temperature range of 283–298 K for glycine-GO. Magnetic GO-Fe(III) (MGO) composites were investigated as adsorbents for a spiked wastewater sample and at low pH, % removal was low due to steric obstacles on large cationic sizes, such as Pb^{2+} (Ain et al. 2020). Their work deduced that the deprotonation of MGO led to an increase in the chelation between heavy metal ions and MGO at high pH. Similarly, Chowdhury et al. (Chowdhury et al. 2018) reported a q_e of 65 mg g^{-1} and a high % removal of As^{3+} within an hour of aqueous spiked samples using a 1-butyl-3-methylimidazolium hexafluorophosphate-MGO (IL-MGO) composite. The use of MGO allows for easy recovery of the adsorbent using a magnetic field and reusability. This was an interesting way to develop effective adsorbents via ternary composites, each component inducing a specific function. In addition, the chitosan-GO composite demonstrated successful elimination of Cr^{4+} from industrial aqueous wastewater and the efficacy was attributed to a synergistic effect between the chelating ability and the large surface area of chitosan and GO, respectively (Y. Liu et al. 2022a, b). In their work, the q_e and the optimal % removal were 24.16 mg g^{-1} and $\sim 97\%$. The studies reviewed here show that most works involving the remediation of heavy metals via adsorption involve artificial matrices through spiking. In addition, there seem to be more adsorption studies on modified GO than on pristine GO.

Understanding the adsorption mechanisms of non-functionalized GO for various contaminants is crucial to optimising its application in real-world scenarios, such as explosive blast mine effluent in the current study. Furthermore, it is essential

to acknowledge the specific characteristics of the pollutant matrices present in wastewater. For example, wastewater sample matrices from industries and explosive blast mine effluent differ from spiked aqueous solutions. Also, different mining operations may result in unique pollutant profiles and associated matrices. This requires qualitative analyses to identify the specific contaminants involved and a possible mitigation strategy tailored to the particular needs of wastewater effluent. Other waste components in wastewater have the potential to influence efficiency and optimal conditions. Therefore, the current work reports on qualitative and quantitative analyses and adsorption of heavy metals from Chegutu mine effluent collected on the 17th of January 2024 using pristine GO. The effluent was collected from a mine located 20 km south-southeast of the town of Chegutu, Mashonaland West, Zimbabwe. This research highlights the feasibility of using pristine GO to remove heavy metals from a natural matrix. This is a step that facilitates the transition from laboratory-spiked samples to real-world samples, and ultimately environmental sustainability.

Materials and methods

Chemicals, materials and instruments

All chemicals were analytical-grade. GO was synthesised from graphite (Sigma Aldrich, < 150 μm , 99.99%) using a modified Tour's method reported elsewhere (Mombeshora 2023). KOH (85%), and HCl (30–33%) were purchased from Glassworld, distilled water was from the University of Zimbabwe plant, and explosive blast mine effluent was collected at a certain mine in Chegutu, a sub-tropical region.

The instruments involved were a BIOBASE atomic absorption spectrometer (AAS, BK- AA32), Rigaku X-ray diffractometer (MiniFlex 600), JEOL scanning electron

microscopy (SEM, JSM 6100 microscope), Shimadzu Fourier transform-infra-red (FT-IR) spectrometer (WQF 520, ASF), magnetic stirrer (EYELA, magnetic stirrer RCH-3), pH meter (Infitek, Benchtop pH-B200E), analytical balance (Mettler AE 240S; Mettler Toledo AG) and vacuum pump (Edwards, SPEEDIVAC).

Characterisation of adsorbent

The morphology of the adsorbent was investigated using SEM. Qualitative analysis of the adsorbent was done through X-ray diffraction (XRD) and the presence of oxygen moieties on the GO surface was carried out with FT-IR spectroscopy.

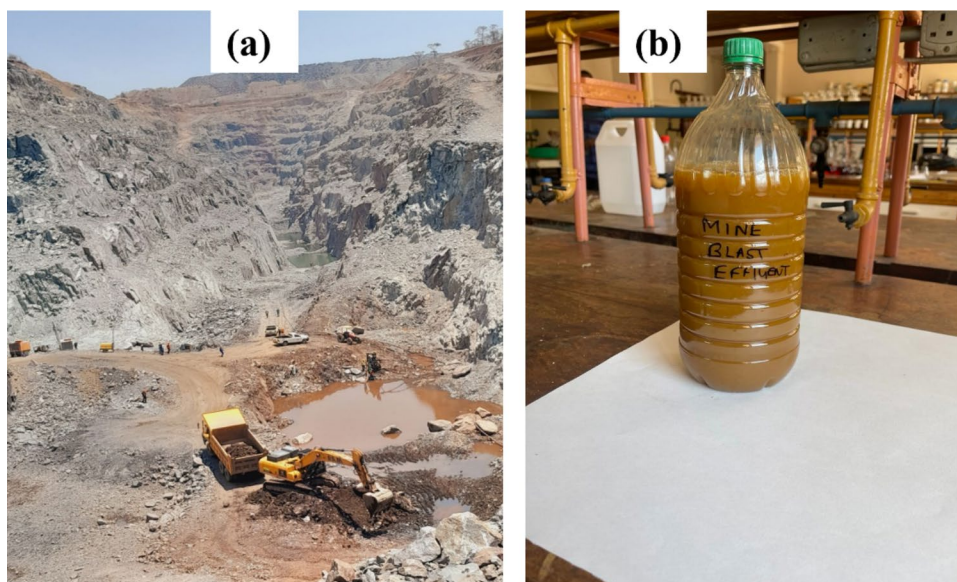
Sample collection

The water sample was collected from a certain sub-tropical mine in Chegutu following a controlled detonation using an ammonium nitrate fuel oil (ANFO) explosive (Fig. 1a). The explosive blast mine effluent was then stored in a thoroughly cleaned plastic bottle under ambient conditions (Fig. 1b).

Qualitative analysis and adsorption studies

Generally, after the mixing stage was performed using a magnetic stirrer, the solids were separated by letting them settle and, thereafter, filtering using a vacuum pump. The sample was then qualitatively analysed using AAS. This was followed by adsorption studies using pristine GO as described in later sections. The AAS step was followed as in qualitative analysis to determine the content of heavy metals remaining in the wastewater after adsorption. Equation 1 was used to calculate the percentage removal of heavy metal ions from explosive mine blast effluent:

Fig. 1 a Sampling site and b sample collected taken to the laboratory



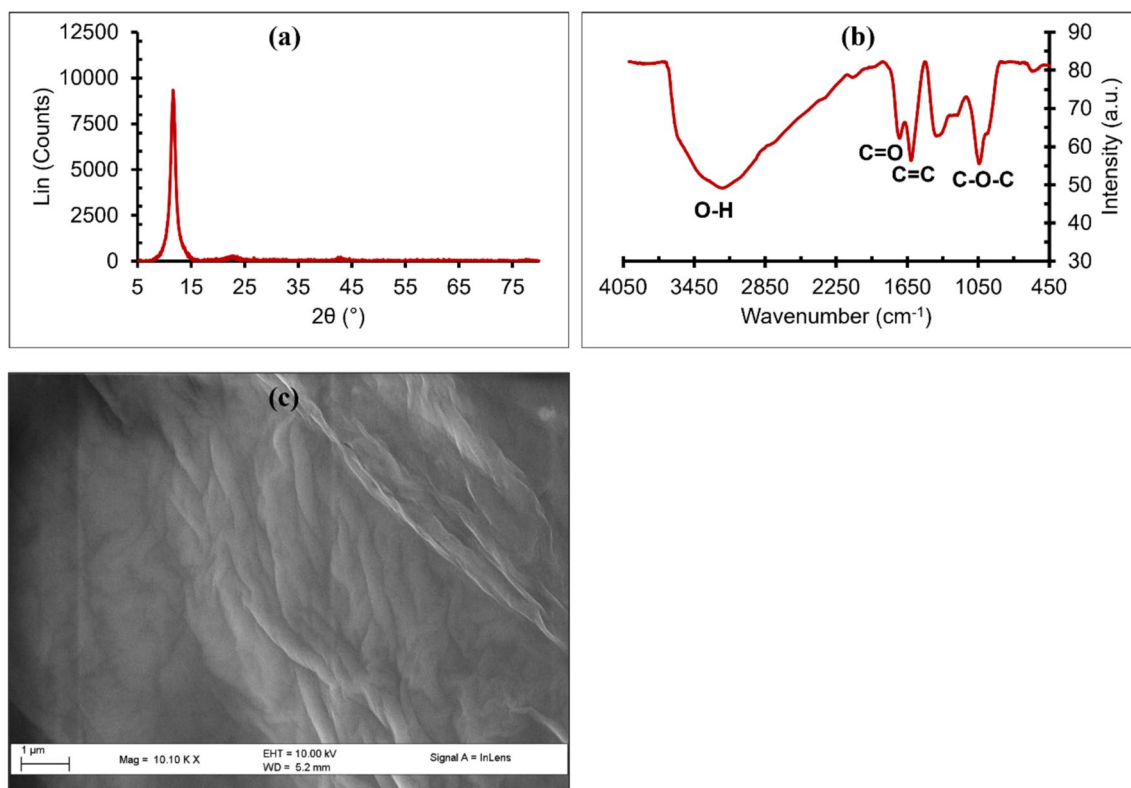


Fig. 2 **a** XRD diffractogram, **b** FT-IR spectra, and **c** SEM micrograph for the GO adsorbent

$$\% \text{ adsorption} = \frac{(C_i - C_e)100\%}{C_i} \quad (1)$$

Where C_i and C_e are the initial and equilibrium amounts of heavy metal in the explosive blast mine effluent in ppm, respectively. In each case, the adsorption amount (q_e) at equilibrium was calculated using Eq. 2, where C_f is the final concentration:

$$q_e = \frac{(C_i - C_f)V}{m} \quad (2)$$

Effect of adsorbent dosage

The masses of pristine GO, namely, 0.1, 0.3, 0.5 and 1 g, were weighed using an analytical balance and transferred to separate beakers each containing 50 mL of explosive blast mine effluent. This was followed by stirring for 0.5 h using a magnetic stirrer at room temperature (25 °C).

Effect of pH

Five different conical flasks were used to determine the initial pH of 50 mL of the explosive blast mine effluent. The pH was then adjusted with 0.1 M KOH and HCl to 2.31, 4.00,

7.00, 9.03 and 12.08. A dose and contact time of 0.5 g and 0.5 h, respectively, were used at room temperature of 25 °C.

Effect of temperature

To determine the effects of temperature on adsorption, the mixture of 0.5 g of adsorbent and 50 mL of explosive blast mine effluent was agitated for 0.5 h at a constant pH of 12.08. The temperatures investigated were 25, 30, 45 and 50 °C.

Contact time

The experiment was carried out at a constant pH, adsorbent dosage and temperature of 12.08, 0.5 g, and 45 °C, respectively, for contact times of 0.5, 1.5 and 2 h.

Adsorption kinetics

To comprehend the suitable adsorption kinetic model, the data were fit into pseudo-first-order (Eq. 3) and pseudo-second-order (Eq. 4) (Parsa & Rezai 2021):

$$\ln(q_e - q_t) = \ln q_t - kt \quad (3)$$

where q_t is the amount of adsorption after a given time, t , in mg g^{-1} , and k is the adsorption rate constant (min^{-1}). The slope of the $\ln(q_e - q_t)$ against y is k .

$$\frac{t}{qt} = \frac{t}{q_e} = \frac{1}{k_2 q_e^2} \quad (4)$$

k^2 is the pseudo-second-order adsorption rate constant in $\text{mg}^{-1} \text{min}^{-1}$.

Isotherms

Isotherms were also studied to appreciate the link between the concentration of adsorbed material and the adsorption capacity of the adsorbent (adsorption at different concentrations). This was done with the aid of the Langmuir isotherm (Eq. 5):

$$\frac{C_e}{q_e} = \frac{1}{K_L q_m} + \frac{C_e}{q_m} \quad (5)$$

where C_e is the equilibrium concentration and is assumed to be equal to C_f in mg L^{-1} , K_L is the Langmuir equilibrium constant and q_m is the saturated monolayer adsorption capacity in mg g^{-1} of the adsorbent.

A dimensionless constant R_L (Eq. 6) is a feature of the Langmuir equation and was used to classify the adsorption process in terms of feasibility (undesirable, linear, irreversible and desirable) (Rezaei 2016).

$$R_L = \frac{1}{1 + K_L C_i} \quad (6)$$

Thermodynamics

For thermodynamic studies, $\Delta_{\text{ads}}H^0$, $\Delta_{\text{ads}}G^0$ and $\Delta_{\text{ads}}S^0$ were the enthalpy change process in kJ mol^{-1} , the Gibbs free energy in kJ mol^{-1} and the entropy change in $\text{kJ mol}^{-1} \text{K}^{-1}$ of adsorption, Eqs. 7a and 7b were used for calculations (Alizadeh Fard & Barkdoll 2018):

$$\Delta_{\text{ads}}G^0 = -R_c T \ln k_c \quad (7a)$$

$$\ln k_c = -\left(\frac{\Delta_{\text{ads}}S^0}{R} - \frac{\Delta_{\text{ads}}H^0}{RT} \right) \quad (7b)$$

where R is the universal gas constant ($8.314 \text{ J mol}^{-1} \text{ K}^{-1}$), T is the wastewater temperature in K and k_c is the equilibrium constant. The k_c is found in the graph of $\ln\left(\frac{q_e}{C_e}\right)$ versus q_e . Equation 7b was used to estimate the values of $\Delta_{\text{ads}}H^0$ and $\Delta_{\text{ads}}S^0$ as *intercept* $\times R$ and *slope* $\times R$ from the Vant Hoff graph, $\ln k_c$ versus $\frac{1}{T}$, and $\Delta_{\text{ads}}G^0$ was calculated from Eq. 7a.

Results and discussion

Adsorbent characterisation

The XRD diffractogram showed a major peak at 2θ of 11.6° (Fig. 2a). This was attributed to 002 graphitic lattices with interlamellar trapped water, which is typical for hydrophilic GO sheets (Mombeshora 2023). The FTIR spectra also confirmed the presence of $\text{C}=\text{C}$ bonds in the graphene framework (Fig. 2b). In addition, the spectra displayed several peaks assigned to various oxygen-containing moieties before and after adsorption (Fig. 2b). This suggests a physisorption process, however, a chemical interaction between the adsorbent and the adsorbate that is not necessarily a chemical bond is feasible. This is possible through electrostatic interactions that cause coordination (Guo et al. 2021; Valentin-Reyes et al. 2019). The adsorbent sheet was also highly wrinkled and this is common in GO samples due to the severe oxidation process (Fig. 2c) (Mombeshora & Nyamori 2017). However, high-quality SEM images after adsorption were difficult to obtain due to severe charging constraints. The cumulative charge, due to the unavailability of grounding pathways, causes image distortions (Flatabo et al. 2017).

Qualitative analysis of wastewater from explosive blast mine effluent

The pH of the wastewater, received from the mine, was 6.74 which is approximately weak acidic in nature. On the other hand, qualitative analysis of explosive blast mine effluent revealed the presence of heavy metals in alarming quantities of 148, 40.70, 12.10 and 0.03 ppm for Cr, Cu, Fe, and Pb, respectively. These findings signify that severe environmental issues can potentially arise from the heavy metal contamination of the mining effluent in the long term. For example, an elevated level of Fe, above 3 ppm, harms aquatic life by disrupting gill function and reproduction (Park et al. 2020). However, Cu levels exceeded the Environmental Protection Agency (EPA) recommended limit of ~ 1.3 ppm for freshwater, thus, also having the potential to be detrimental to aquatic life (Manne et al. 2022). Even at low concentrations, Pb is still concerning as a result of its high toxicity. Exposure to Pb can lead to major health problems in people and animals, affecting the nervous system, blood, and kidneys (Wani et al. 2015). The highest concentration of Cr is of significant concern to the environment. Cr exists in several forms that are sometimes highly toxic and carcinogenic (Sharma et al. 2022). Further studies are crucial to identify the specific type of chromium present. Hence, qualitative and quantitative analysis motivated the development of an effluent treatment strategy and pristine GO was investigated as a potential adsorbent for heavy metals in sub-tropical regions.

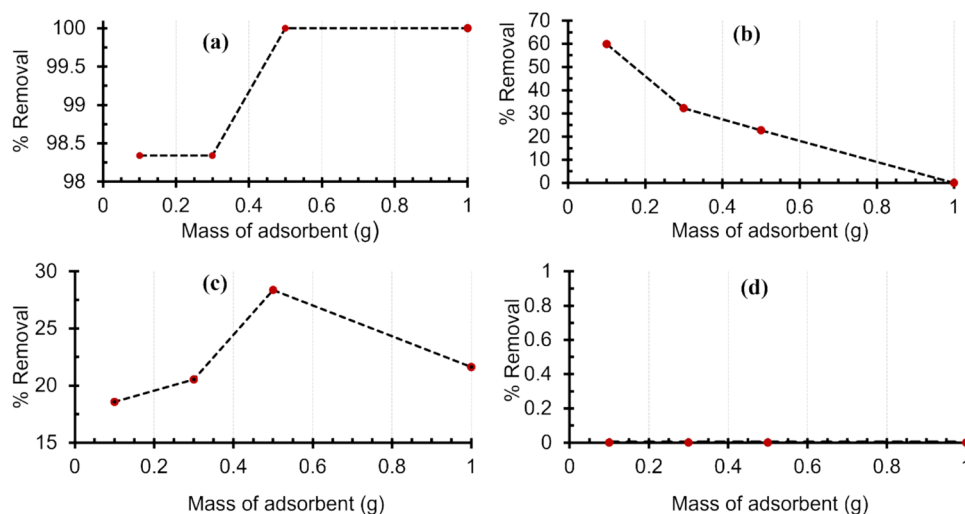


Adsorbent dose requirements for water resource recovery

Variations in adsorbent dose from 0.1 to 1 g displayed different impacts on the % removal efficiency of each metal (Fig. 3). This is attributed to the sample matrix and the forms of metal in the wastewater mine effluent. For Fe, the % removal was high at 0.1 g and reached 100% at 0.5 g (Fig. 3a). The highest % removal of Cu was at the dose of 0.1 g and decreased with the adsorbent's mass (Fig. 3b). This means that pristine GO had the highest affinity for Fe followed by Cu at a low adsorbent dose. The increase in % removal slightly improved for Cr, reached a maximum at 0.5 g and had a higher attraction to the surface of GO than Cu at high doses (Fig. 3c). The decrease, beyond 0.5 g, could indicate the decrease of adsorbate on the GO (Wu et al. 2012). This logically agrees with the literature in that more adsorbent provides more surfaces for adsorption (Khalilha et al. 2021).

Pb displayed the least adsorption tendencies to the active sites of GO under weak acidic conditions (Fig. 3d). This adsorption trend in this study can be rationalised by the position of the heavy metals in the periodic in which the smaller cationic-sized metal is expected to have a higher affinity for the negatively charged oxygen moieties on GO. This is consistent with other studies that deduced varying degrees of cation affinity for functional groups of adsorption sites (Phatthanakittiphong & Seo 2016). However, Cr was ranked third rather than first under weak acidic conditions. This could be due to the form of Cr or the sample matrix in the explosive blast mine effluent under weak acidic conditions. As the dosage increased, the adsorption equilibrated due to the saturation of binding sites. Therefore, considering the efficacy and economic issues, the optimal adsorbent dosage for the studies of the explosive blast mine effluent of the mine can be estimated to be 0.5 g.

Fig. 3 Adsorbent dosage against % removal of **a** Fe, **b** Cu, **c** Cr, and **d** Pb at pH of 6.74



Investigating the pH requirements for the effluent treatment

An interesting interplay between pH and heavy metal removal efficiency was observed (Fig. 4). Excellent removal efficiencies of Cu, Fe and Pb, exceeded ~86%, as the pH increased (Fig. 4a, b and d). This could be rationalised by the change in surface charges on GO. At high pH, GO becomes more negatively charged, thus, the attraction to cationic forms increases through electrostatic interactions, which in turn promotes adsorption (Liu et al. 2012). The consistently high % removal above neutral pH (> 98%) for Cu, Fe, and Pb is ascribed to the strong affinity of the present metal forms for the GO surface and leads to effective adsorption regardless of surface charge (Kang et al. 2020; Nguyen et al. 2021; Pyrzynska 2023). For Pb, % removal under acidic, neutral, and basic conditions was uniquely different from that under natural weak acidic conditions (0%). Possibly this could be due to an unfavourable chemical transformation of Pb that hinders adsorption on GO.

In contrast, removal of Cr fluctuated as pH increased, suggesting a weaker interaction between Cr cation and GO surface moieties (Fig. 4c). This could be because surface charge changes have been reported to repel other cation forms (Liu et al. 2012). This agrees with the dose–effect study, which suggests that Cr form in the explosive blast mine effluent influenced the adsorption process. Cr has a variety of oxidation states and exhibits more sensitive behaviour to pH changes. For example, based on the pH and concentration of the effluent, the three primary forms of Cr(VI) are Cr, CrO_4^{2-} and $\text{Cr}_2\text{O}_7^{2-}$ as well as HCrO_4^- (Gao et al. 2023; Liao et al. 2022). For the 1–7 pH range, the predominant form of Cr(VI) in the effluent is HCrO_4^- and is transformed to $\text{Cr}_2\text{O}_7^{2-}$ at pH greater than 7 (Gao et al. 2023; Liao et al. 2022). At pH greater than 9, Cr(VI) in effluents is only present as CrO_4^{2-} (Gao et al. 2023; Liao et al. 2022). Under basic conditions, HCrO_4^- is less favourable for adsorption

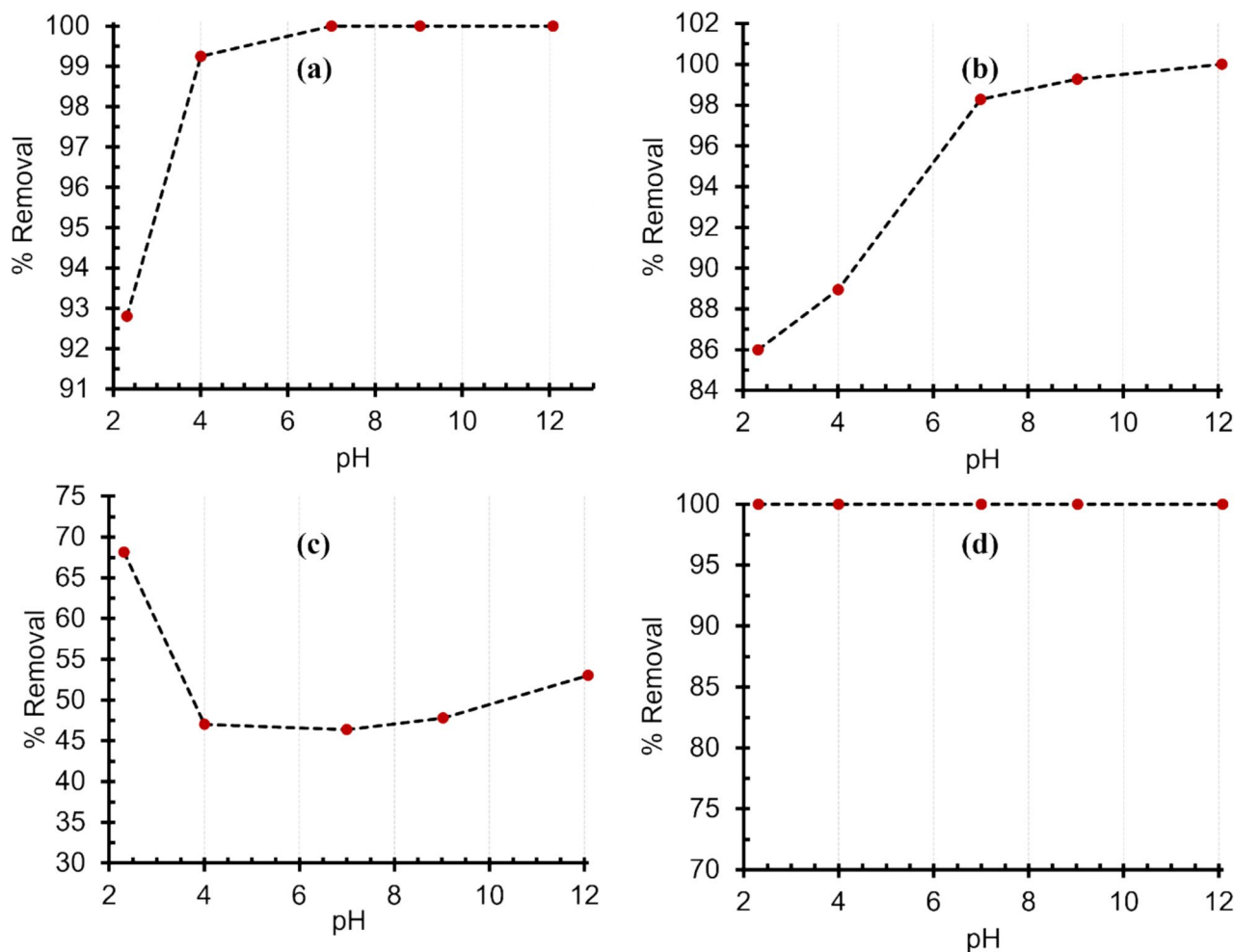


Fig. 4 Influence of pH effect on removal efficiency for **a** Fe, **b** Cu, **c** Cr, and **d** Pb

on the highly negative GO surface compared to other cation forms. Lastly, considering all detected heavy metals in the sample matrix of the explosive blast effluent of the mine, the basic conditions, particularly the pH of ~12, are optimum for effluent treatment.

Temperature determination for optimum remediation

Studying the temperature effect helps determine the underlying thermodynamic parameters, such as enthalpy and entropy, which govern the adsorption process. The temperature range was selected to preserve the bulk of the GO adsorbent nature. The % removal of Cu, Fe, and Pb was consistently 100% across all temperatures tested at pH 12.08. This indicates their excellent and consistent adsorption on the GO surface in the studied temperature range. This was ascribed to enhanced mobility at high temperatures that increased the kinetic energy in the Brownian motion of Fe and Cu ions. This promotes faster movement and more frequent collisions

with the GO surface, leading to its efficient adsorption (Guo et al. 2021). Furthermore, increasing temperature enhances the ionisation of the oxygen-containing functional groups on GO to form more binding sites for Fe and Cu (Guo et al. 2021). The % of Cr removal was highest at 25 °C and deteriorated to an approximately constant value with increasing temperature (Fig. 5). Therefore, considering all metals in the explosive blast mine effluent, the study infers that the treatment can be optimally performed at an ambient temperature of ~25 °C. Therefore, GO adsorbents support energy-saving treatment methodologies for explosive blast mine effluent.

The contact time prerequisites for water resource recovery

For Pb, a contact time of 0.5 h was sufficient to achieve 100% removal (Table 1). A rapid initial uptake of Fe and Cu was observed (over 99% removal) and 0.5 h was sufficient for the cations to diffuse through the solution and encounter the available adsorption sites on the GO (Table 1). This supports

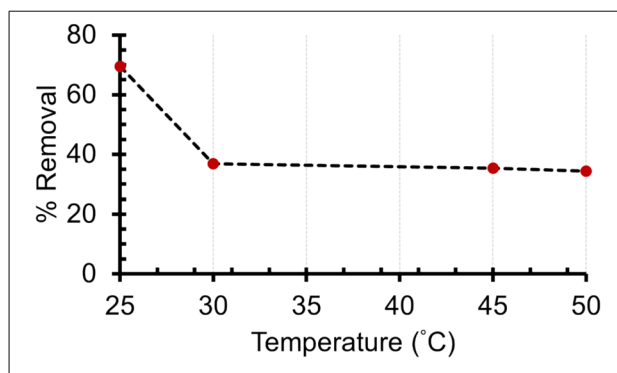


Fig. 5 Effect of temperature on the removal efficiency of Cr using GO adsorbent at pH 12.08

the earlier deduced strong and rapid GO/metal attraction. This possibly means that the use of GO adsorbents for the current explosive blast mine effluent is potentially economical. However, the % removal of Cr after contact times of 0.5, 1 and 2 suggest possible desorption at prolonged contact times (Table 1). Slower uptake of Cr suggests weaker or more complex interactions that may be reversible.

Investigating the mode adsorption from a kinetic perspective

Kinetic studies were performed to determine the variables that affect the rate of adsorption. Studying the adsorption kinetics with pseudo-first-order and pseudo-second-order models provides a valuable starting point for understanding the governing kinetics for the removal of heavy metals by adsorbents. Pseudo-first-order infers slow diffusion of pollutants onto limited binding sites of GO, whereas, pseudo-second-order suggests control of the adsorption rate through chemisorption of heavy metals onto GO surface (Wang 2012). The kinetic data for Fe and Cu suggest that adsorption followed pseudo-second-order kinetics and, thus, was through a chemisorption process (Table 2).

Table 1 Effect of contact time on cation adsorption at pH of 12.08

Contact time (h)	Concentration (ppm)				% Removal			
	Fe	Cu	Cr	Pb	Fe	Cu	Cr	Pb
0	12.10	40.70	148.00	0.03	0.00	0.00	0.00	0.00
0.5	0.08	0.02	99.00	0.00	99.33	99.95	33.10	100
1.5	0.01	0.00	102.00	0.00	99.98	100	31.08	100
2	0.00	0.00	107.40	0.00	100	100	27.43	100

Table 2 Kinetic adsorption parameters for heavy metal removal

Heavy metal	Pseudo-first-order			Pseudo-second-order		
	q_e (mg g ⁻¹)	K_1	R^2	q_e (mg g ⁻¹)	K_2	R^2
Fe	1.39	5.00×10^{-5}	0.78	1.00	108.76	1.00
Cu	30.66	6.66×10^{-8}	0.79	83.75	1.26	1.00
Cr	1.08	1.83×10^{-4}	0.99	106.72	0.00	0.99

Chemical interactions are feasible via cations that coordinate with the lone pairs on oxygen-containing moieties of GO. This suggests that adsorption was governed by the adsorbent dose and concentration of adsorbate in wastewater from the explosive blast mine effluent. Hence, this explains the observations under the dose–effect studies. Interestingly, the maximum adsorption capacity obtained through pseudo-second order was 83.75 mg g^{-1} for Cu which agreed with the one determined experimentally in the contact time batch adsorption experiments (83.72 mg g^{-1}).

For Cr, both pseudo-first-order and pseudo-second-order kinetics are feasible, with the pseudo-second-order slightly preferred (R^2 in Table 2). This is an interesting variation of Cu and Fe which is feasibly rationalised by a variation of cation forms in the mine blast effluent. Another possible rationale is that the adsorption and desorption of Cr followed pseudo-second- and pseudo-first-order kinetics, respectively. In this case, desorption is influenced only by the amount of Cr already adsorbed on the GO surface. Additionally, the theoretical q_e determined via pseudo-second-order, 106.72 mg g^{-1} , was in close agreement with the result of the batch adsorption of contact time of 100.82 mg g^{-1} . The q_e agreements validated the experimental results with the theoretical approaches. In summary, the regression coefficients (R^2) values infer that the adsorption of all three cations followed pseudo-second-order. Therefore, the adsorption process was controlled by chemical interactions between oxygen moieties on GO and heavy metal cations.

Test for monolayer adsorption mechanism

The Langmuir model was employed to characterise the adsorption process for Cu, Fe and Cr since most graphene-based adsorbent follows a monolayer adsorption mechanism (Sarmiento et al. 2023) and the kinetics of the current study inferred a chemisorption process. The Langmuir model assumes a uniform distribution of adsorption sites and no

Table 3 Langmuir adsorption isotherm parameters for heavy metal removal

Heavy metal ion	Langmuir isotherm		
	K_L	R_L	R^2
Fe	76.86	0.0011	0.13
Cu	19.98	0.0012	0.96
Cr	0.001	0.9850	0.93

interaction between the surface of the adsorbent and the adsorbate (Zhang et al. 2018).

By determining the intercept and slope values from the $\frac{C_e}{q_e}$ against C_e graph, K_L and q_m values were determined as the intercept and $\frac{1}{slope}$, respectively. Furthermore, the R^2 values were determined (Table 3) and suggest that Fe did not follow the monolayer adsorption mechanism (large deviation from 1). The adsorption process for Cu was relatively close to that of the monolayer adsorption process with some slight deviations. This suggests the possibility of other surface coverage mechanisms different from most graphene-based adsorbents when used in cation removal in the current sample matrix. This is practically sound because cations can be removed by being trapped between GO nanosheets. Dimensionless separation parameter (R_L) was employed to explain the Langmuir isotherm expressed in Eq. 6. If R_L is > 1 , 1 , 0 and $0 < R_L < 1$ then means that the adsorption is undesirable, linear, irreversible and favourable (feasibility of the reaction), respectively (Mahvi & Heibati 2010). The R_L values suggest that the removal of Fe, Cu, and Cr was spontaneous (Table 3), hence, pristine GO is suitable for the treatment of the blast effluent from the Chegutu mine.

Study of adsorption feasibility through thermodynamics

Understanding thermodynamics is crucial in optimising the treatment process of the explosive blast mine effluent containing various contaminants. Thermodynamic parameters, such as $\Delta_{ads}G$, help determine whether the adsorption process is spontaneous. A negative $\Delta_{ads}G$ for Cu, Fe and Cr infers that their adsorption onto the GO surface was spontaneous (Table 4). This means that they were readily bound to GO, promoting ease

of removal from explosive blast mine effluent. The spontaneity improved with the temperature for Cu and Fe.

$\Delta_{ads}H$ and $\Delta_{ads}S$ provide insight into the energetics of the adsorption process (Cordova Estrada et al. 2021). Furthermore, $\Delta_{ads}S$ inferred spontaneous adsorption for Cu and Fe, while Cr was spontaneous in desorption (Table 4). This was corroborated by trends observed with earlier parameters, particularly on the temperature effect. The positive values of $\Delta_{ads}H$ for Fe and Cu implied that the adsorption process was endothermic, thus, explaining the increase in % removal with temperature. On the other hand, $\Delta_{ads}H$ for Cr was exothermic, therefore, high temperature promoted desorption from the pristine GO surface (Table 4).

To compare performance with literature values, selected q_m values were taken from the literature with similar carbon adsorbent applied in real-world natural samples (Table 5). It should be noted that most reports involved spiked samples with no competitive adsorption effects. Except for Pb adsorption, q_m values in the current work (Table 5), were superior to recently reported oxidised carbon-based adsorbents. The inferior Pb affinity, of the current pristine GO adsorbent, could have been influenced by competitive adsorption effects. Notable variations in heavy metal adsorption capacities emanate from the sample matrix nature and the differences in adsorbent physicochemical characteristics such as textural characteristics, nature, and content of functional moieties on the adsorbent surface. The unique nature of the sample matrix of the current blast mine effluent is a significant factor in the accuracy of the comparison with other adsorbents in the literature.

Chemical precipitation is one of the methods currently in use in removing heavy metals from effluents, however, unlike the adsorption process, it adds extra cost from chemical requirements and constant corrosion of equipment, and hence, it will most likely not be adopted in the sub-tropical regions. Furthermore, the chemical precipitation process might generate products, such as metal sulfides, that are difficult to handle and some hydroxides (e.g., Cu and Cr) are insoluble (Zhang & Duan 2020). Therefore, adsorption demonstrated using GO, in the current work, is superior in this regard. Coagulation treatment using alum, eggshells, and ferromagnetite showed an optimum contaminant removal of almost 100% from industrial

Table 4 Langmuir adsorption parameters at different temperatures

Heavy metal	Temperature (K)	K_L	$\Delta_{ads}G$ (kJ mol ⁻¹)	$\Delta_{ads}H$ (kJ mol ⁻¹)	$\Delta_{ads}S$ (J K ⁻¹ mol ⁻¹)	R^2
Fe	303	1242.80	-17.95	+20.61	+127.65	0.79
	318	2487.65	-20.67			
	323	2487.65	-21.00			
Cu	303	2032.94	-19.19	+30.37	+163.76	0.90
	318	4067.94	-21.97			
	323	4067.94	-22.31			
Cr	303	1.13	-0.32	-0.96	-2.01	-0.89
	318	1.20	-0.47			
	323	1.08	-0.20			



Table 5 Comparison of the adsorption capacity of heavy metals in the natural sample waste matrix using carbon-based adsorbents

Adsorbent	Metal ion species	Adsorption conditions				q_m (mg g ⁻¹)	Ref
		Dose (g L ⁻¹)	pH	T (K)	C_i (ppm)		
Carbon foam	Cr	5	2.2	–	93.25	17.48	(Lee et al. 2016)
Graphene nanoplatelets	Cr	2	7.55	298	2.08	2	(Konradt et al. 2024)
Pristine GO	Cr	10	6.7	298	148	100.82	This work
Oxidised nano-activated carbon	Cu	2	7.8	301	1.18	13.23	(Elkady et al. 2020)
Chicken bone charcoal-sodium dodecyl sulfonate-Fe	Cu	–	3.0	298	50	15.06s	(Niu et al. 2021)
Carbon foam	Cu	5	2.2	–	36.16	6.92	(Lee et al. 2016)
Pristine GO	Cu	10	6.7	298	40.70	83.72	This work
Chitosan	Fe	0.355	3.5	303	55	40	(Hu et al. 2009)
Activated carbon	Fe	12	5.4	300	25.2	2.08	(Fosu et al. 2022)
Oxidised nano activated carbon	Fe	2	7.8	301	3.2	7.52	(Elkady et al. 2020)
Pristine GO	Fe	10	6.7	298	12.10	26.08	This work
Oxidised cotton hull	Pb	0.085	7.4	–	85	27.65	(Yahya et al. 2020)
Oxidised MWCNT	Pb	2	–	298	100	27	(Gusain et al. 2019)
Oxidised nano activated carbon	Pb	2	7.8	301	1.86	11.63	(Elkady et al. 2020)
Pristine GO	Pb	10	6.7	298	0.03	0.10	This work

wastewater with a 20 mg L⁻¹ dose (Precious Sibiyi et al. 2021). Interestingly, the optimal dose of GO adsorbent in the current work is 10 g L⁻¹ with 100% Fe removal, which is comparable to their work with high dose requirements (Table 5). Therefore, the current pristine GO as an adsorbent is comparable in terms of cost-effectiveness and is facile relative to current mine wastewater treatments, such as coagulation, as materials can also be derived from waste biomass. Advantageously, the adsorption method is being critically considered for heavy metal removal due to its simple designs of infrastructure, high efficiency at affordable prices, and suitability on both small and large scales (Gusain et al. 2019, 2020). Most importantly, in the context of the mine where the study was carried out, the effluent is currently being discharged without undergoing treatment. Therefore, the current study highlights the feasible and practical remediation strategy that the mine and other sub-tropical mines can adopt.

Conclusion

Firstly, the study qualitatively and quantitatively investigated the existence of heavy metals in wastewater from a natural explosive blast mine effluent. Secondly, the work explored the use of pristine GO as an adsorbent for the removal of heavy metal contaminants. The qualitative analysis successfully identified a range of heavy metals in explosive blast mine effluent which were 12.10, 40.70, 148 and 0.03 ppm for Fe, Cu, Cr and Pb, respectively, and all at alarming concentrations. The temperature, pH, contact time, and

adsorbent dose were optimised as 12.08, 0.5 h, 25 °C and 0.5 g, respectively, for the explosive blast mine effluent. The excellent removal of heavy metals within 0.5 h in a basic medium at room temperature and the use of pristine GO through a spontaneous process demonstrated its potential as an economical adsorbent. Therefore, pristine GO is suitable for treating ANFO explosive blast mine effluent in water resource recovery facilities. Further research should include the regeneration capacity of the GO adsorbent and this study can be potentially supported by speciation studies to establish the species of heavy metals in the explosive blast mine effluent.

Acknowledgements The authors thank the Materials Formulations and Energy Research Group, University of Zimbabwe, for supporting this work and providing the necessary research infrastructure. ETM acknowledges the support from the Faculty of Engineering and the Built Environment and the School of Chemical and Metallurgical Engineering, University of the Witwatersrand and the University of Pretoria.

Author contributions FRK: Conceptualization, Formal analysis and Investigation, and Writing – original draft. HH: Writing – review & editing, Validation, and Resources. ETM: Conceptualization, Methodology, Formal analysis, Writing – review & editing, Validation, Resources, Project administration, and Funding acquisition.

Funding Open access funding provided by University of Pretoria.

Data availability Data and sample materials are available on request.

Declarations

Conflicts of Interest The authors declare that they have no conflict of interest.

Open Access This article is licensed under a Creative Commons Attribution 4.0 International License, which permits use, sharing,

adaptation, distribution and reproduction in any medium or format, as long as you give appropriate credit to the original author(s) and the source, provide a link to the Creative Commons licence, and indicate if changes were made. The images or other third party material in this article are included in the article's Creative Commons licence, unless indicated otherwise in a credit line to the material. If material is not included in the article's Creative Commons licence and your intended use is not permitted by statutory regulation or exceeds the permitted use, you will need to obtain permission directly from the copyright holder. To view a copy of this licence, visit <http://creativecommons.org/licenses/by/4.0/>.

References

- Ain Q-U, Farooq MU, Jalees MI (2020) Application of magnetic graphene oxide for water purification: heavy metals removal and disinfection. *J Water Process Eng* 33:101044. <https://doi.org/10.1016/j.jwpe.2019.101044>
- Alizadeh Fard M, Barkdoll B (2018) Magnetic activated carbon as a sustainable solution for removal of micropollutants from water. *Int J Environ Sci Technol* 16(3):1625–1636. <https://doi.org/10.1007/s13762-018-1809-5>
- Anegbe B, Ifijen IH, Maliki M, Uwidia IE, Aigbodion AI (2024) Graphene oxide synthesis and applications in emerging contaminant removal: a comprehensive review. *Environ Sci Eur* 36(1):15. <https://doi.org/10.1186/s12302-023-00814-4>
- Bailey BL, Smith LJD, Blowes DW, Ptacek CJ, Smith L, Sego DC (2013) The Diavik waste rock project: persistence of contaminants from blasting agents in waste rock effluent. *Appl Geochem* 36:256–270. <https://doi.org/10.1016/j.apgeochem.2012.04.008>
- Borges ME, de Paz CH, Gutiérrez M, Esparza P (2023) Photocatalytic removal of water emerging pollutants in an optimized packed bed photoreactor using solar light. *Catalysts* 13(6):1023. <https://doi.org/10.3390/catal13061023>
- Cao K, Tian Z, Zhang X, Wang Y, Zhu Q (2023) Green preparation of graphene oxide nanosheets as adsorbent. *Sci Rep* 13(1):9314. <https://doi.org/10.1038/s41598-023-36595-2>
- Chowdhury T, Zhang L, Zhang J, Aggarwal S (2018) Removal of arsenic(III) from aqueous solution using metal organic framework-graphene oxide nanocomposite. *Nanomaterials (Basel)* 8(12):1062. <https://doi.org/10.3390/nano8121062>
- Cordova Estrada AK, Cordova Lozano F, Lara Díaz RA (2021) Thermodynamics and kinetic studies for the adsorption process of methyl orange by magnetic activated carbons. *Air, Soil Water Res* 14:117862212110133. <https://doi.org/10.1177/11786221211013336>
- Dubey SP, Nguyen TTM, Kwon Y-N, Lee C (2015) Synthesis and characterization of metal-doped reduced graphene oxide composites, and their application in removal of *Escherichia coli*, arsenic and 4-nitrophenol. *J Ind Eng Chem* 29:282–288. <https://doi.org/10.1016/j.jiec.2015.04.008>
- Ebenebe P, Shale K, Sedibe M, Tikilili P, Achilonu M (2018) South African mine effluents: heavy metal pollution and impact on the ecosystem. *Int J Chem Sci* 15(4):198
- ElBastamy E, Ibrahim LA, Ghandour A, Zelenakova M, Vranayova Z, Abu-Hashim M (2021) Efficiency of natural clay mineral adsorbent filtration systems in wastewater treatment for potential irrigation purposes. *Sustainability* 13(10):5738. <https://doi.org/10.3390/su13105738>
- Elkady M, Shokry H, Hamad H (2020) New activated carbon from mine coal for adsorption of dye in simulated water or multiple heavy metals in real wastewater. *Materials (Basel)* 13(11):2498. <https://doi.org/10.3390/ma13112498>
- El-taweel RM, Mohamed N, Alrefaey KA, Husien S, Abdel-Aziz AB, Salim AI, Mostafa NG, Said LA, Fahim IS, Radwan AG (2023) A review of coagulation explaining its definition, mechanism, coagulant types, and optimization models; RSM, and ANN. *Current Res Green Sustain Chem* 6:100358. <https://doi.org/10.1016/j.crgsc.2023.100358>
- Flatabo R, Coste A, Greve MM (2017) A systematic investigation of the charging effect in scanning electron microscopy for metal nanostructures on insulating substrates. *J Microsc* 265(3):287–297. <https://doi.org/10.1111/jmi.12497>
- Fosu S, Kwakye E, Arthur SK, Osei LB (2022) Characterisation of a rehabilitated tailings dam mine water as a potential acid mine drainage and removal of heavy metals using locally produced activated carbon. *Ghana Min J* 23(2):154–168. <https://doi.org/10.4314/gm.v22i1.3>
- Gao F, Zhang L, Yang L, Zhou X, Zhang Y (2023) Structural properties of graphene oxide prepared from graphite by three different methods and the effect on removal of Cr(VI) from aqueous solution. *Nanomaterials (Basel)* 13(2):279. <https://doi.org/10.3390/nano13020279>
- Guo T, Bulin C, Ma Z, Li B, Zhang Y, Zhang B, Xing R, Ge X (2021) Mechanism of Cd(II) and Cu(II) adsorption onto few-layered magnetic graphene oxide as an efficient adsorbent. *ACS Omega* 6(25):16535–16545. <https://doi.org/10.1021/acsomega.1c01770>
- Gusain R, Kumar N, Fosso-Kankeu E, Ray SS (2019) Efficient removal of Pb(II) and Cd(II) from industrial mine water by a hierarchical MoS₂/SH-MWCNT nanocomposite. *ACS Omega* 4(9):13922–13935. <https://doi.org/10.1021/acsomega.9b01603>
- Gusain R, Kumar N, Ray SS (2020) Recent advances in carbon nanomaterial-based adsorbents for water purification. *Coord Chem Rev* 405:213111. <https://doi.org/10.1016/j.ccr.2019.213111>
- Hu J, Chen C, Zhu X, Wang X (2009) Removal of chromium from aqueous solution by using oxidized multiwalled carbon nanotubes. *J Hazard Mater* 162(2–3):1542–1550. <https://doi.org/10.1016/j.jhazmat.2008.06.058>
- Jahan N, Roy H, Reaz AH, Arshi S, Rahman E, Firoz SH, Islam MS (2022) A comparative study on sorption behavior of graphene oxide and reduced graphene oxide towards methylene blue. *Case Stud Chem Environ Eng* 6:100239. <https://doi.org/10.1016/j.csee.2022.100239>
- Kang Y-G, Chi VuH, Chang Y-Y, Chang Y-S (2020) Fe(III) adsorption on graphene oxide: a low-cost and simple modification method for persulfate activation. *Chem Eng J* 387:124012. <https://doi.org/10.1016/j.cej.2020.124012>
- Khalilha S, Marforio TD, Kovtun A, Mantovani S, Bianchi A, Luisa Navacchia M, Zambianchi M, Bocchi L, Boulanger N, Iakunov A, Calvaresi M, Talyzin AV, Palermo V, Melucci M (2021) Defective graphene nanosheets for drinking water purification: adsorption mechanism, performance, and recovery. *FlatChem* 29:100283. <https://doi.org/10.1016/j.flatc.2021.100283>
- Konradt D, Schroden D, Hagemann U, HeideImann M, Rohns HP, Wagner C, Konradt N (2024) Kinetics of direct reaction of vanadate, chromate, and permanganate with graphene nanoplatelets for use in water purification. *Nanomaterials (Basel)* 14(2):140. <https://doi.org/10.3390/nano14020140>
- Lee CG, Song MK, Ryu JC, Park C, Choi JW, Lee SH (2016) Application of carbon foam for heavy metal removal from industrial plating wastewater and toxicity evaluation of the adsorbent. *Chemosphere* 153:1–9. <https://doi.org/10.1016/j.chemosphere.2016.03.034>
- Liao J, Wu Y, Chen X, Yu H, Lin Y, Huang K, Zhang J, Zheng C (2022) Light-triggered oxidative activity of chromate at neutral pH: A colorimetric system for accurate and on-site detection of Cr(VI) in natural water. *J Hazard Mater* 440:129812. <https://doi.org/10.1016/j.jhazmat.2022.129812>



- Liu L, Liu S, Zhang Q, Li C, Bao C, Liu X, Xiao P (2012) Adsorption of Au(III), Pd(II), and Pt(IV) from aqueous solution onto graphene oxide. *J Chem Eng Data* 58(2):209–216. <https://doi.org/10.1021/je300551c>
- Liu X, Zhang J, Huang X, Zhang L, Yang C, Li E, Wang Z (2022a) Heavy metal distribution and bioaccumulation combined with ecological and human health risk evaluation in a typical urban plateau lake, southwest China. *Front Environ Sci* 10:814678. <https://doi.org/10.3389/fenvs.2022.814678>
- Liu Y, Shan H, Zeng C, Zhan H, Pang Y (2022b) Removal of Cr(VI) from wastewater using graphene oxide chitosan microspheres modified with α -FeO(OH). *Materials (Basel)* 15(14):4909. <https://doi.org/10.3390/ma15144909>
- Liu M, Wang Y, Wu Y, Liu C, Liu X (2023) Preparation of graphene oxide hydrogels and their adsorption applications toward various heavy metal ions in aqueous media. *Appl Sci* 13(21):11948. <https://doi.org/10.3390/app132111948>
- Maharana M, Sen S (2021) Magnetic zeolite: A green reusable adsorbent in wastewater treatment. *Materials Today: Proceedings* 47:1490–1495. <https://doi.org/10.1016/j.matpr.2021.04.370>
- Mahdhi N, Alsaari NS, Amari A, Osman H, Hammami S (2023) Enhancement of the physical adsorption of some insoluble lead compounds from drinking water onto polylactic acid and graphene oxide using molybdenum disulfide nanoparticles: theoretical investigation. *Front Phys* 11:1159306. <https://doi.org/10.3389/fphy.2023.1159306>
- Mahvi AH, Heibati B (2010) Removal efficiency of Azo dyes from textile effluent using activated carbon made from walnut wood and determination of isotherms of acid Red18. *J Health* 1:7–15
- Manne R, Kumaradoss MMRM, Iska RSR, Devarajan A, Mekala N (2022) Water quality and risk assessment of copper content in drinking water stored in copper container. *Appl Water Sci* 12(3):27. <https://doi.org/10.1007/s13201-021-01542-x>
- Mishra SR, Roy P, Gadore V, Ahmaruzzaman M (2023) A combined experimental and modeling approach to elucidate the adsorption mechanism for sustainable water treatment via In_2S_3 -anchored chitosan. *Sci Rep* 13(1):18051. <https://doi.org/10.1038/s41598-023-45506-4>
- Mombeshora ET (2023) Understanding solvothermal reductive reactions of graphene oxide in boron and ammonia solutions. *J Mater Sci: Mater Electron* 34(6):521. <https://doi.org/10.1007/s10854-023-09955-x>
- Mombeshora ET, Muchuveni E (2023) Dynamics of reduced graphene oxide: synthesis and structural models. *RSC Adv* 13(26):17633–17655. <https://doi.org/10.1039/d3ra02098c>
- Mombeshora ET, Nyamori VO (2017) Physicochemical characterization of graphene oxide and reduced graphene oxide composites for electrochemical capacitors. *J Mater Sci: Mater Electron* 28(24):18715–18734. <https://doi.org/10.1007/s10854-017-7821-6>
- Najafi F, Moradi O, Rajabi M, Asif M, Tyagi I, Agarwal S, Gupta VK (2015) Thermodynamics of the adsorption of nickel ions from aqueous phase using graphene oxide and glycine functionalized graphene oxide. *J Mol Liq* 208:106–113. <https://doi.org/10.1016/j.molliq.2015.04.033>
- Nguyen MT, Zhang J, Prabhakaran V, Tan S, Baxter ET, Shutthanandan V, Johnson GE, Rousseau R, Glezakou VA (2021) Graphene oxide as a Pb(II) separation medium: has part of the story been overlooked? *JACS Au* 1(6):766–776. <https://doi.org/10.1021/jacsau.0c00075>
- Niu C, Li S, Zhou G, Wang Y, Dong X, Cao X (2021) Preparation and characterization of magnetic modified bone charcoal for removing Cu^{2+} ions from industrial and mining wastewater. *J Environ Manage* 297:113221. <https://doi.org/10.1016/j.jenvman.2021.113221>
- Obey G, Adelaide M, Ramaraj R (2022) Biochar derived from non-customized matamba fruit shell as an adsorbent for wastewater treatment. *J Bioresour Bioprod* 7(2):109–115. <https://doi.org/10.1016/j.jobab.2021.12.001>
- Park H, Noh K, Min JJ, Rupa C (2020) Effects of toxic metal contamination in the tri-state mining district on the ecological community and human health: a systematic review. *Int J Environ Res Public Health* 17(18):6783. <https://doi.org/10.3390/ijerph17186783>
- Parsa N, Rezaei H (2021) Removal of lead ions from aqueous solutions using melamine-modified nano graphene oxide. *Avic J Environ Health Eng.* 7(2):55–65
- Peng W, Li H, Liu Y, Song S (2017) A review on heavy metal ions adsorption from water by graphene oxide and its composites. *J Mol Liquids* 230:496–504
- Phatthanakitiphong T, Seo GT (2016) Characteristic evaluation of graphene oxide for bisphenol a adsorption in aqueous solution. *Nanomaterials (Basel)* 6(7):128. <https://doi.org/10.3390/nano6070128>
- Precious Sibiya N, Rathilal S, Kweiner Tetteh E (2021) Coagulation treatment of wastewater: kinetics and natural coagulant evaluation. *Molecules* 26(3):698. <https://doi.org/10.3390/molecules26030698>
- Pyrzynska K (2023) Preconcentration and removal of Pb(II) ions from aqueous solutions using graphene-based nanomaterials. *Materials (Basel)* 16(3):1078. <https://doi.org/10.3390/ma16031078>
- Radu VM, Vişdea AM, Ivanov AA, Alexe VE, Dincă G, Cetean VM, Filiiuță AE (2023) Research on the closure and remediation processes of mining areas in Romania and approaches to the strategy for heavy metal pollution remediation. *Sustainability* 15(21):15293. <https://doi.org/10.3390/su152115293>
- Rezaei H (2016) Biosorption of chromium by using *Spirulina* sp. *Arab J Chem* 9(6):846–853. <https://doi.org/10.1016/j.arabjc.2013.11.008>
- Sarmiento V, Lockett M, Sumbarda-Ramos EG, Vazquez-Mena O (2023) Effective removal of metal ion and organic compounds by non-functionalized rGO. *Molecules* 28(2):649. <https://doi.org/10.3390/molecules28020649>
- Sharma P, Singh SP, Parakh SK, Tong YW (2022) Health hazards of hexavalent chromium (Cr (VI)) and its microbial reduction. *Bioengineered* 13(3):4923–4938. <https://doi.org/10.1080/21655979.2022.2037273>
- Sitko R, Musielak M, Zawisza B, Talik E, Gagor A (2016) Graphene oxide/cellulose membranes in adsorption of divalent metal ions. *RSC Adv* 6(99):96595–96605. <https://doi.org/10.1039/c6ra21432k>
- Valentin-Reyes J, Garcia-Reyes RB, Garcia-Gonzalez A, Soto-Regalado E, Cerino-Cordova F (2019) Adsorption mechanisms of hexavalent chromium from aqueous solutions on modified activated carbons. *J Environ Manage* 236:815–822. <https://doi.org/10.1016/j.jenvman.2019.02.014>
- Wang X (2012) Nanomaterials as sorbents to remove heavy metal ions in wastewater treatment. *J Environ Anal Toxicol* 02(07):1000154. <https://doi.org/10.4172/2161-0525.1000154>
- Wani AL, Ara A, Usmani JA (2015) Lead toxicity: a review. *Interdiscip Toxicol* 8(2):55–64. <https://doi.org/10.1515/intox-2015-0009>
- Wu W, Yang Y, Zhou H, Ye T, Huang Z, Liu R, Kuang Y (2012) Highly efficient removal of Cu(II) from aqueous solution by using graphene oxide. *Water Air Soil Pollut* 224(1):1372. <https://doi.org/10.1007/s11270-012-1372-5>
- Yahya MD, Yohanna I, Auta M, Obayomi KS (2020) Remediation of Pb (II) ions from Kagara gold mining effluent using cotton hull adsorbent. *Sci Afr* 8:e00399. <https://doi.org/10.1016/j.sciaf.2020.e00399>
- Zhang Y, Duan X (2020) Chemical precipitation of heavy metals from wastewater by using the synthetic magnesium hydroxy carbonate. *Water Sci Technol* 81(6):1130–1136. <https://doi.org/10.2166/wst.2020.208>
- Zhang Y, Yao S, Zhang M, Zhou X, Mei H, Zeng F (2018) Prediction of adsorption isotherms of multicomponent gas mixtures in tight porous media by the oil-gas-adsorption three-phase vacancy



solution model. *Energy Fuels* 32(12):12166–12173. <https://doi.org/10.1021/acs.energyfuels.8b02762>

Zhang S, Li W, Tang H, Huang T, Xing B (2022) Revisit the adsorption of aromatic compounds on graphene oxide: Roles of oxidized

debris. *Chem Eng J* 450:137996. <https://doi.org/10.1016/j.cej.2022.137996>